CHAPTER 11

OPTICAL BAND GAP OF Sb_2Te_3 AND Sb_2Te_3 BASED CRYSTALS

When an alloy is made of two semiconductors, it is expected that the energy gap of the alloy will assume a value intermediate between the gaps of the two pure semiconductors and that the gap will vary in proportion to the composition. However, the rate of change of the energy gap with composition depends on the nature of the lowest conduction-band valley. Thus, Ge and Si form a solid solution, $Ge_{1-x}Si_x$, continuously miscible over the whole compositional range $0 < x < 1$[1]. However the energy gap of the alloy does not vary linearly with the composition. The deviation from linearity may be accounted for by the formation of band tails due to the random perturbation of the lattice by the minority atoms. Ternary alloys between II-VI compounds preserve a direct gap over the whole compositional range. In $ZnS_{1-x}Se_x$ the energy gap varies linearly with composition; whereas $ZnS_{1-x}Te_x$ and $ZnSe_{1-x}Te_x$ have an anomalously high nonlinear dependence, which still lacks an explanation[2]. In the system $Hg_{1-x}Cd_xTe$ the energy gap varies linearly between 1.6 eV for CdTe and – 0.14 eV for HgTe[3]. The negative sign of the energy gap signifies that the conduction and valence bands overlap, transforming the semiconductor into a semimetal. The ability to tailor the energy gap to such small values has made this alloy very important for infrared detection. Hence, band gap variation can be done by either varying the concentration or the type of incorporated elements in a semiconducting material.

The fundamental absorption, which manifests itself by a rapid rise in absorption, can be used to determine the energy gap of the semiconductor. Apart from absorption measurements, the band gap can also be deduced from the photoconductivity measurements, conductivity measurements, transmission

measurements and so on. The transport properties of Sb_2Te_3, Sb_2Te_3-Bi_2Te_3 and Sb_2Te_3-In_2Te_3 solid solutions have been extensively studied in a number of papers[4-10]. However, only little attention has been devoted to the optical band gap of these crystals. Jaschke[11] found the forbidden band width of Sb_2Te_3 to be 0.19 eV. It has been found by others using the optical measurements to be 0.3 eV and 0.21 eV[12,13]. The differences between the values of the forbidden band width are due to the large error in the measurements because of the high carrier density which in turn is due to the presence of excess antimony in Sb_2Te_3[14]. The fundamental band gap of Sb_2Te_3-Bi_2Te_3 system has been measured by a number of authors. Rosi et al.[15] have infered that the energy band gap decreases as Sb_2Te_3 is alloyed into Bi_2Te_3 since the intrinsic resisitivity decreases with increasing Sb_2Te_3 content. Testardi and Wiese[16] have observed minima in the values of thermal energy gaps at 33.3% and 66.7% Sb_2Te_3 and attribute this to a tighter packing of atoms in ordered alloys. Airapetiants and Efimova[17] postulate an overlap of the conduction and valence bands in Sb_2Te_3, resulting in an apparent band gap of zero for the terminal compound. Their postulation, however, does not agree with the values of the optical energy gap 0.30eV reported by Black et al.[12] for Sb_2Te_3. Smith et al.[18] calculated the thermal energy gaps for the Bi_2Te_3-Sb_2Te_3 system from the resistivity vs temperature data. They observed that E_g diminishes in an essentially linear fashion from 0.16 eV, for pure Bi_2Te_3, to 0.12 eV at 24.2 mole% Sb_2Te_3 in both slowly crystallized and quenched materials. E_g remains approximately constant across 24.2% to 66.7 mole% Sb_2Te_3 for slowly crystallized materials but continues to drop for quenched materials. Sehr et al.[13] have determined the optical energy gaps indicating indirect transitions from the transmittance and reflectance measurements. They found that the energy gap increases with increasing Sb content in Bi_2Te_3-Sb_2Te_3 system in contrast to the thermal energy gaps, a result attributed in part to the increasing degeneracy

of the charge carriers. They have also reported the temperature dependence of the optical band gap for the same system. Kohler and Freudenberger[19] have deduced the energy gap between the two different valence band maxima which are occupied by high hole concentrations by making use of the Shubnikov-de Haas effect and found it to be approximately constant in the whole range of the mixed crystal system of $(Bi_{1-x}Sb_x)_2Te_3$. Stolzer et al.[20] have investigated IR transmission spectra of $(Bi_{1-x}Sb_x)_2Te_3$ single crystals with x = 0.5, 0.7, 0.9 near the absorption edge at 84 and 300 K and have calculated the energy gap and the phonon energies. Kroutil et al.[21] have analysed the reflectance spectra in the plasma-resonance frequency region and transmittance spectra in the infrared region for $In_xSb_{2-x}Te_3$ crystals and have used the results to show that the value of high frequency dielectric constant ε_∞ decreases with increasing indium content. Lostak et al.[22] have observed an increase in the width of the optical gap with increasing indium content and have explained this on the basis of simultaneous action of Moss Burstein effect and variation of gap width of mixed semiconducting crystals. However detailed explanation was not possible.

The present study includes the evaluation of the fundamental band gap of $Bi_xSb_{2-x}Te_3$ (x = 0, 0.2, 0.5, 1) and $In_{0.2}Sb_{1.8}Te_3$ from the absorption measurements. The absorption measurements of the samples were made on the Michelson Series FT-IR spectrometer (BOMEM, Canada). The general description of the spectrometer[23] is given below.

THE SPECTROMETER

The spectrometer is a self contained unit consisting of one sample compartment and a sealed interferometer compartment. The sample compartment is enclosed in a purge cover provided with access doors. Mirrors are used to channel infrared radiation to the sample position and to the detector. The instrument compartment contains a stabilized infrared light source, the Michelson interferometer, and infrared-transmitting "beamsplitter", a Helium-Neon laser for

measurement of scan position, power supplies and electronic assemblies. The cast aluminum compartment is sealed to prevent the entry of dust and moist air, which can erode the beamsplitter. The specifications of the instruments are listed in Table 1. There are no routine adjustments to be made on the spectrometer.

PRINCIPLE OF OPERATION

FT-IR (Fourier Transform InfraRed) spectrometer possesses several advantages over dispersive spectrometers. Instead of spatially separating the optical frequencies, the FT-IR spectrometer modulates all wavelengths simultaneously with distinct modulation frequencies for each wavelength. This is done by means of a variable interference effect created by separating the incoming beam into two parts, then introducing a path difference, and finally recombining the beam. The resulting beam intensity recorded as a function of optical path difference, with an IR sensitive detector, is called an interferogram. Computing the Fourier transform of the interferogram yields the infrared spectrum. Fig. 1 illustrates these principles. The photograph of the FT-IR spectrometer is shown in Fig. 2.

SAMPLE PREPARATION

The preparation of sample surfaces is important for the IR measurement. It has been found for some semiconductors that good mechanically polished surfaces give the reflecting power expected on the basis of the optical constants of the bulk material, and thus true bulk properties can be deduced from transmission measurements made on samples a few microns in thickness. On the other hand, there are crystals for which good polished surfaces are difficult to obtain. For some crystals, specimens can be obtained by cleaving, giving surfaces suitable for optical measurements. The surface condition is more important for reflection measurements, especially when the radiation penetrates only a small depth on account of high absorption. It has long been known that mechanically polished surfaces of metals give results different from those obtained on electrolytically polished surfaces.[24] Mechanical polishing damages the crystal at the surface and

TABLE 1

Spectrometer Specification

Source	Glowbar, high intensity and power stabilized.
Wavenumber precision	0.01 cm^{-1} controlled with an internal HeNe laser.
Detector	High speed Deuterated triglycine sulfate (DTGS)
Resolution	4 cm^{-1} fixed
Beam splitter	Proprietary ZnSe design
Wavenumber range	6000 cm^{-1} to 510 cm^{-1}

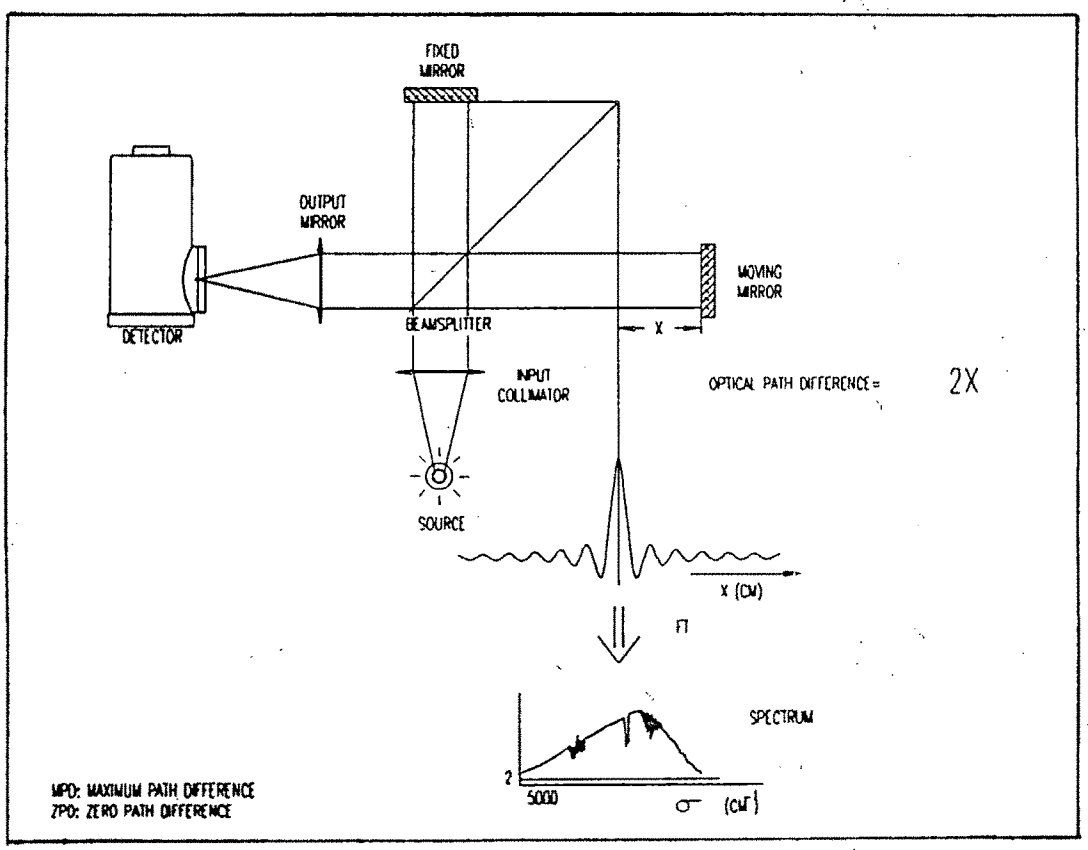

Fig. 1. Principle of operation of FT-IR spectrometer

Fig. 2. F.T.I.R Spectrometer

produces an amorphous layer. The sensitivity to surface condition is largely responsible for the discrepancies in the results obtained by different investigators for the same metals. Experimental indications are that electropolished surfaces may give results reflecting the bulk properties[25,26]. However, because of the high carrier density of about 10^{19} cm^{-3} [27] in $(Bi_{1-x}Sb_x)_2Te_3$, it is very difficult to carry out transmission measurements. Further, good preparation techniques and experimental equipments are required. Hence in the present case, the KBr pressed disk technique was used because of it simplicity and its ability to produce good spectra from very small samples. Further, using KBr as a matrix has following advantages.

1) High transmission of radiation
2) Low sintering pressure
3) High purity and anhydrous
4) Chemically stable

The crystalline powder sample (14 mg) and spectroscopic grade dry KBr powder matrix (300 mg) was ground to a particle size of 5 μm and was mixed thoroughly. Then it was transferred to an evacuable die of about 1 cm diameter and evacuated at 10^{-2} Torr for at least 2 minutes. Then a pressure of about 2 ton was applied for a minimum of 2 minutes. The pressure and vacuum was released. Then the spectrum was obtained using the pellet with a minimum of exposure to atmospheric moisture.

EXPERIMENTAL RESULTS

The optical absorption was measured in the wave number range 510 cm^{-1} to 4000 cm^{-1} and the absorption spectrum was recorded. By analysing the spectrum, absorption coefficient was calculated as a function of photon energy. Since in the pelettized samples, the material thickness is undetermined, an arbitary thickness was assumed. This would of course not give absolute absorption coefficient. However, the relative variations only are significant for the purpose of evaluating optical band gap.

The dependence of the absorption coefficient α on photon energy E near the absorption edge is given by

$$\alpha = A\,(E - E_g)^n$$

where A is a slowly varying function which may be regarded as a constant over the narrow range considered and n is a number which depends on the nature of the transition. n is equal to 1/2 for a direct allowed transition, 3/2 for a direct forbidden transition, 2 for an indirect allowed transition and 3 for an indirect forbidden transition.

The plots of $(\alpha h\nu)^2$ vs $h\nu$ were used to evaluate the optical band gaps. These plots are shown in Fig. 3-7 for $Bi_xSb_{2-x}Te_3$ (x = 0, 0.2, 0.5, 1) and $In_{0.2}Sb_{1.8}Te_3$ respectively. The plots are observed to be linear in the region of strong absorption near the fundamental absorption edge. Hence by extrapolating the linear portion to $(\alpha h\nu)^2 = 0$, the band gap was evaluated. The values of the band gaps obtained are given in Table 2.

DISCUSSION

It is observed that there is a decrease in the band gap with the increase of Bi concentration in Sb_2Te_3 and even upon incorporating In into Sb_2Te_3. While the results obtained for $Bi_xSb_{2-x}Te_3$ (x = 0, 0.2, 0.5, 1) are in agreement with the simple model assuming that the value of E_g for substitutional solid solutions of Sb_2Te_3 and Bi_2Te_3 lies between the values of E_g of the pure binary crystals [Sb_2Te_3 = 0.3 eV[12] and Bi_2Te_3 = 0.16 eV[28]], the results of In incorporated Sb_2Te_3 do not follow the model. Lostak et al.[22] have observed an increase in the width of the optical gap of Sb_2Te_3 with increasing indium content which has been explained on the basis of simultaneous action of Moss Burstein effect and variation of gap width of mixed semiconducting crystals. According to Harbecke and Lautz[29] the value of E_g of In_2Te_3 is 1.05 eV as evaluated from optical absorption measurements. Hence its solid solution with Sb_2Te_3 is expected to have the band gap in the intermediate range as per the simple model stated above.

Fig. 3. Plot of $(\alpha h\upsilon)^2$ vs $h\upsilon$ for Sb_2Te_3

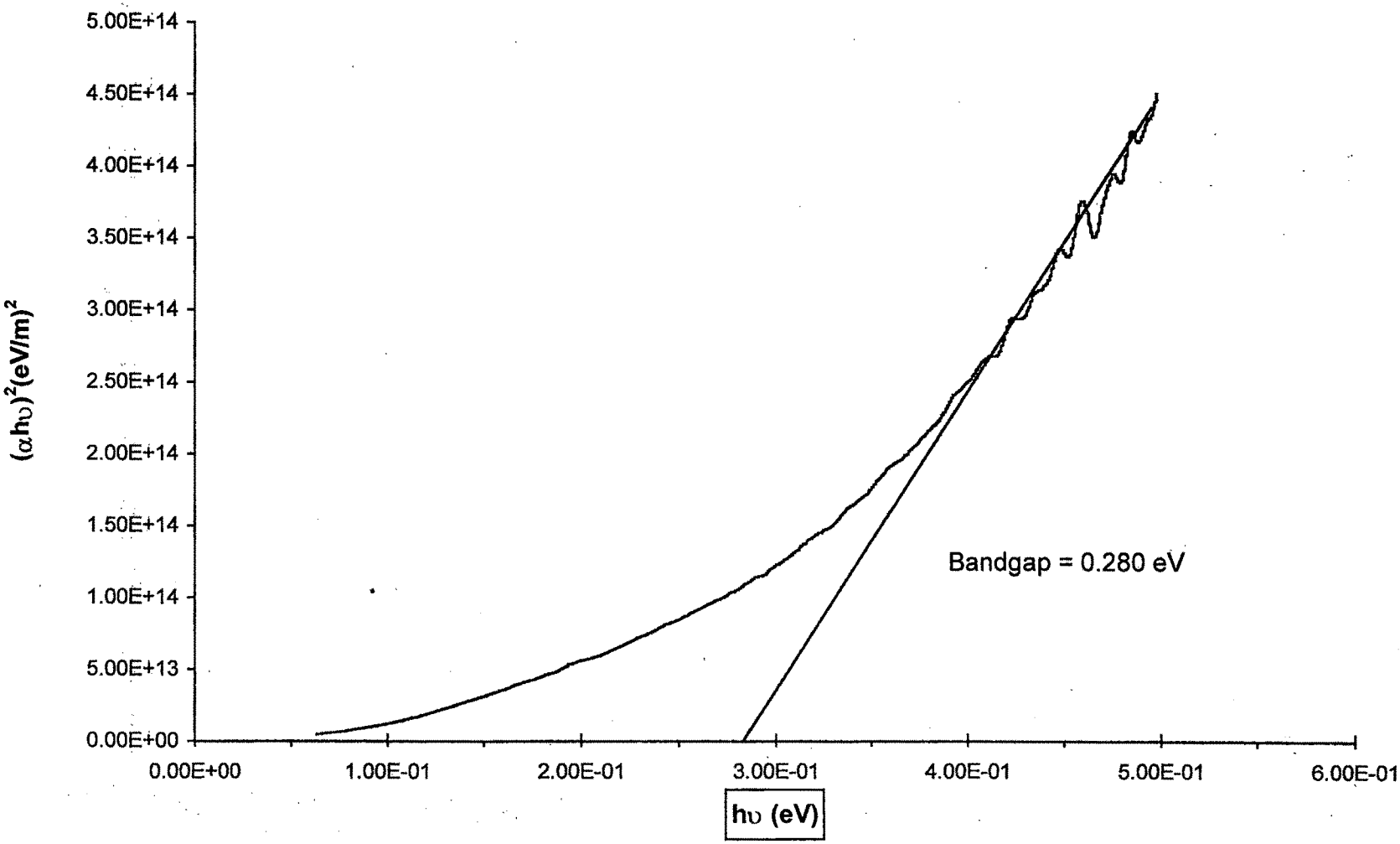

Fig. 4. Plot of $(\alpha h\upsilon)^2$ vs $h\upsilon$ for $Bi_{0.2}Sb_{1.8}Te_3$

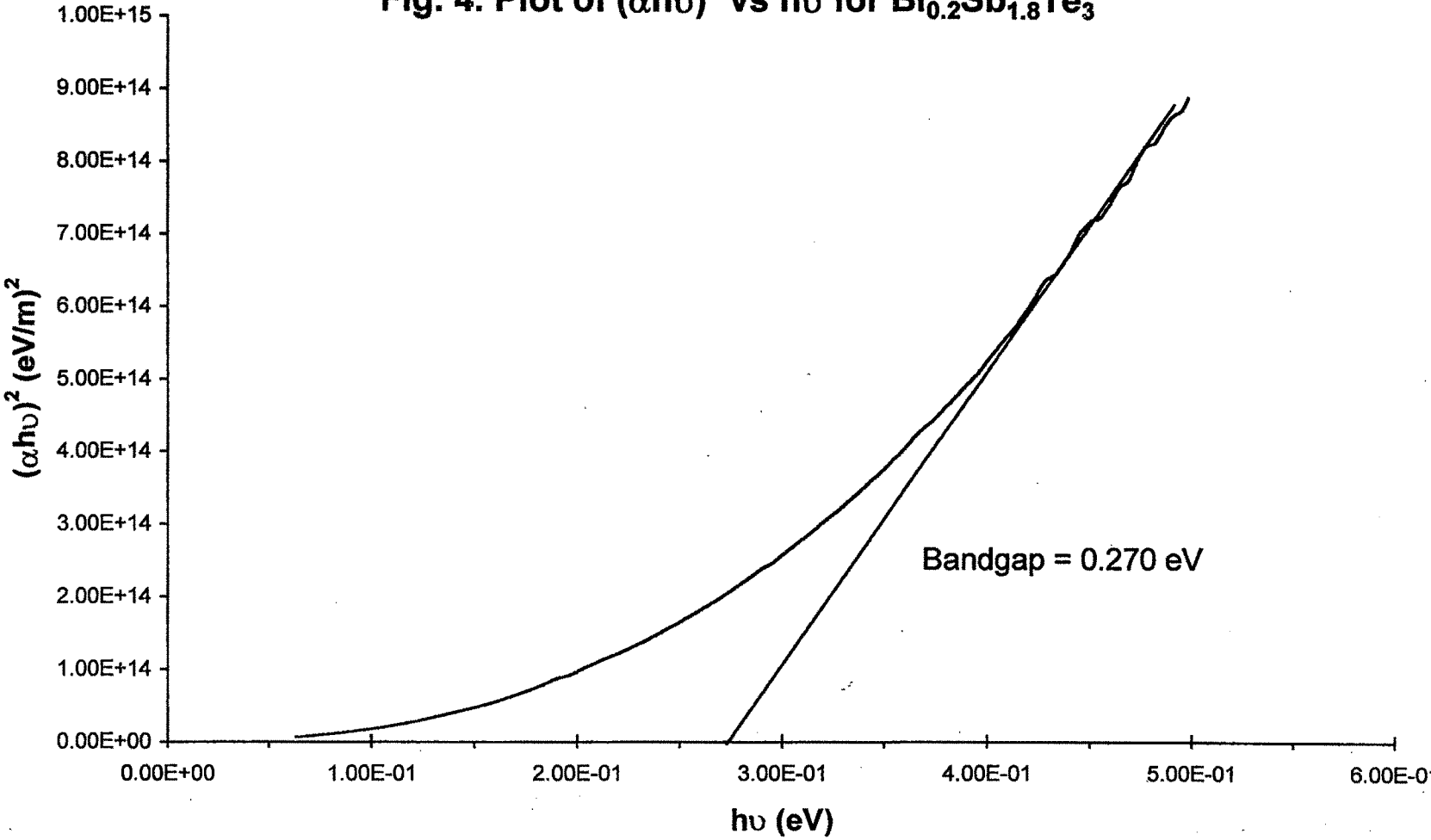

Fig. 5. Plot of $(\alpha h\upsilon)^2$ vs $h\upsilon$ for $Bi_{0.5}Sb_{0.5}Te_3$

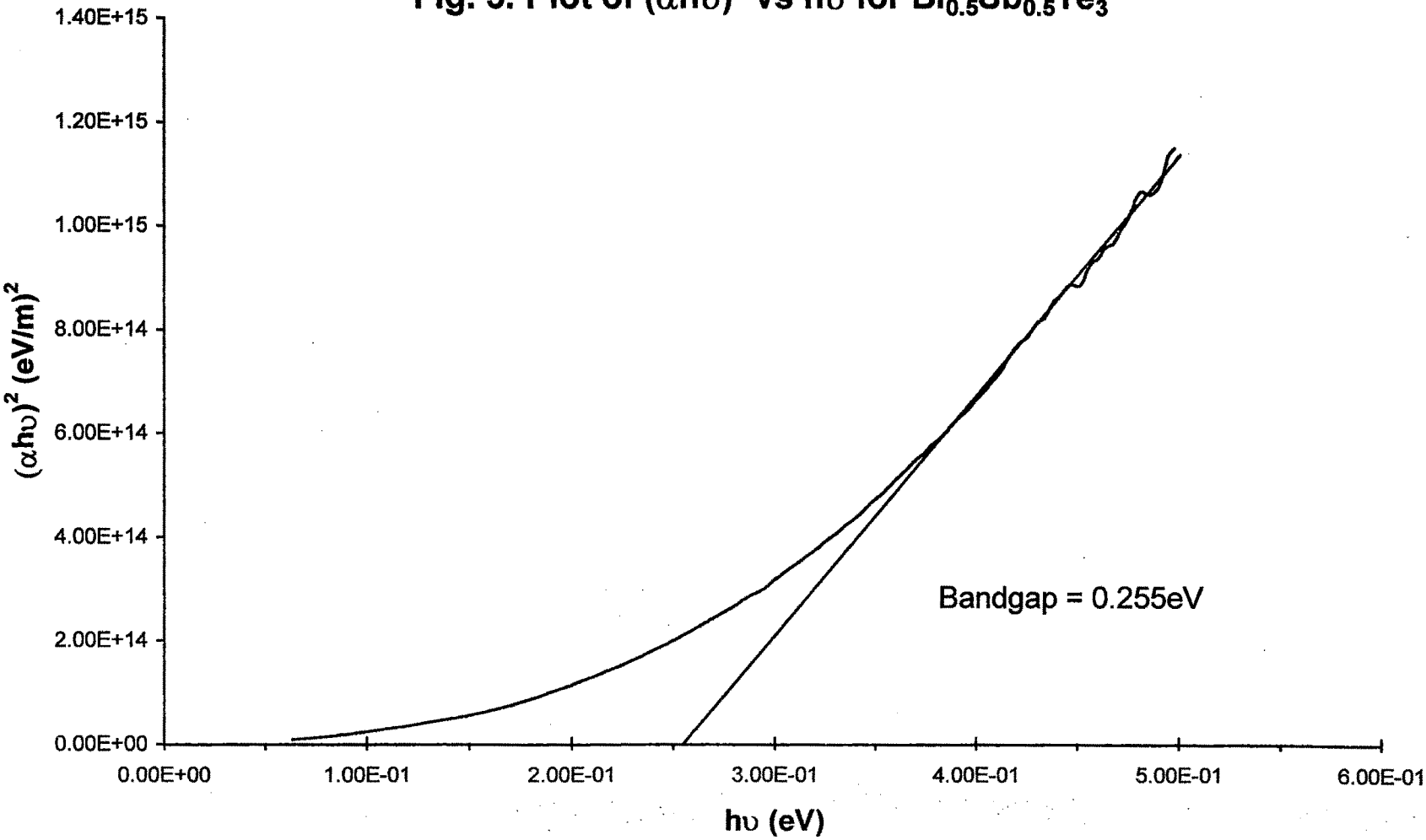

Fig. 6. Plot of $(\alpha h\upsilon)^2$ vs $h\upsilon$ for $BiSbTe_3$

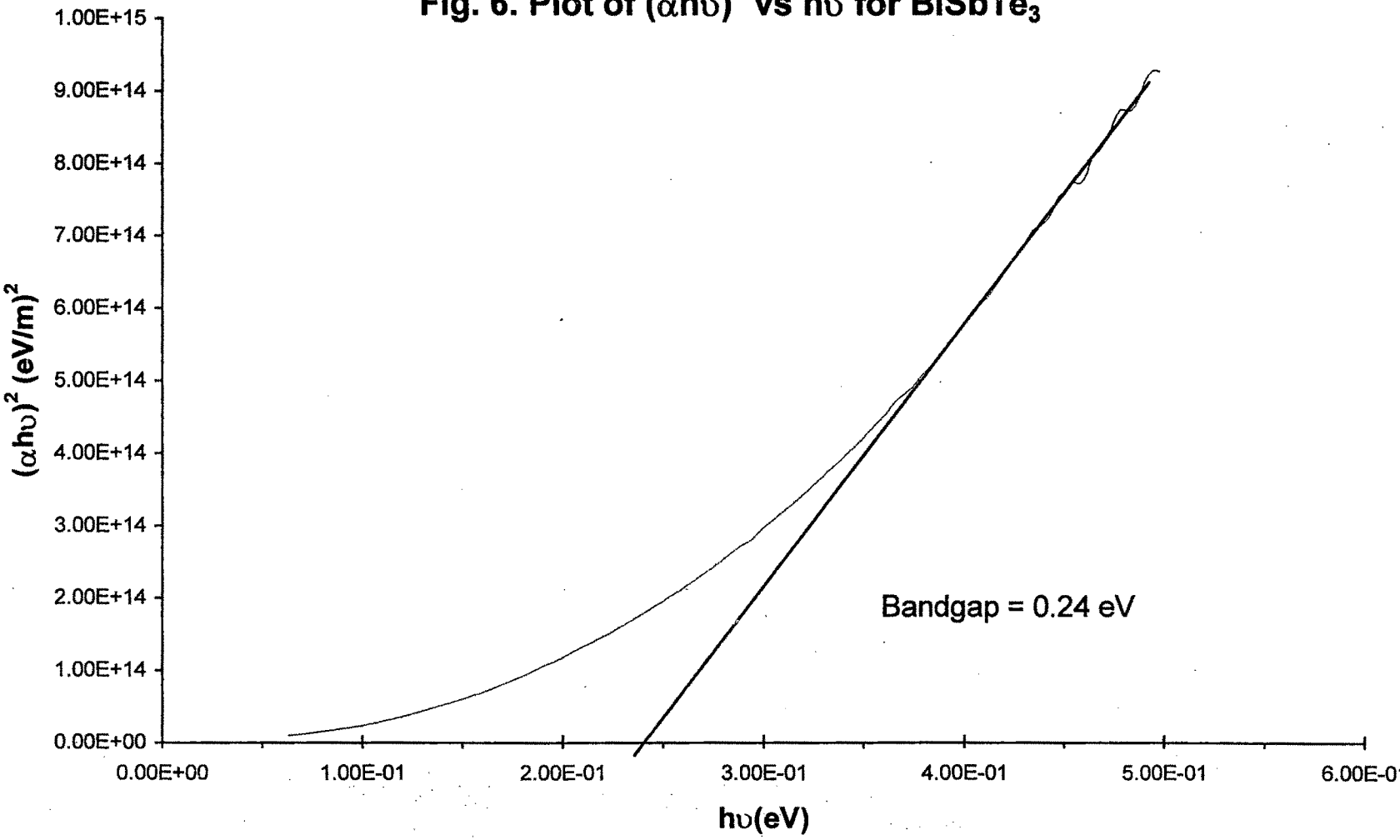

Fig. 7. Plot of $(\alpha h\upsilon)^2$ vs $h\upsilon$ for $In_{0.2}Sb_{1.8}Te_3$

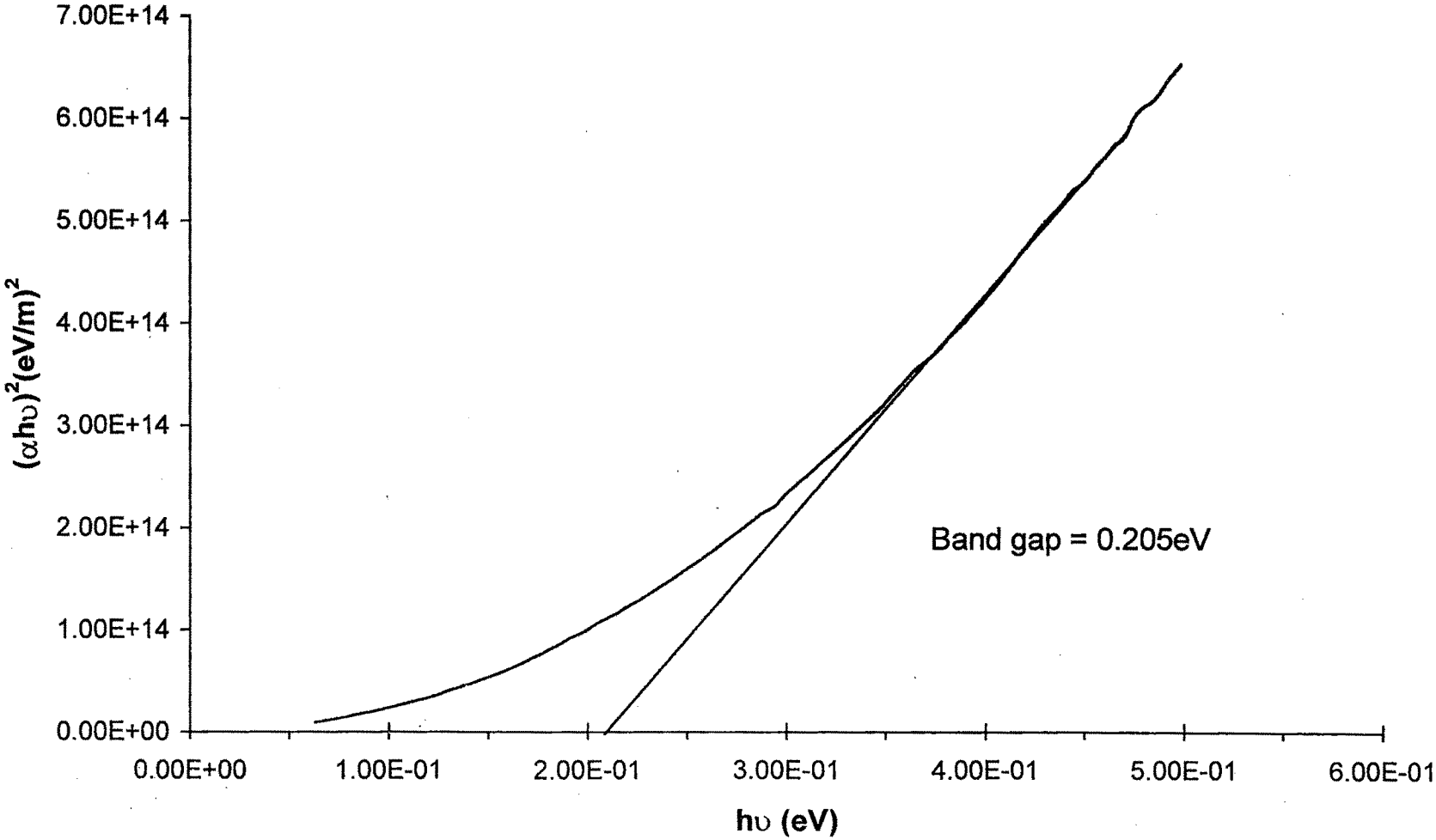

TABLE 2

Optical Band Gap Values

Crystal	Direct gap (eV)
Sb_2Te_3	0.280
$Bi_{0.2}Sb_{1.8}Te_3$	0.270
$Bi_{0.5}Sb_{1.5}Te_3$	0.255
$BiSbTe_3$	0.240
$In_{0.2}Sb_{1.8}Te_3$	0.205

However it has been observed that the results obtained are not in accordance with this expectation. The results obtained can have a plausible explanation as follows:

The incorporation of impurity atoms into Sb_2Te_3 can be realized in several ways:

(a) The impurity atoms enter as interstitials within the structural layers;

(b) They occupy positions in the Sb sublattice;

(c) They occupy Te^{II} sites in the Te sublattice with octahedral coordination to the Sb atoms;

(d) They occupy Te^{I} sites in the Te sublattice;

(e) They enter the Van der Waal's gaps in the layered structured of Sb_2Te_3.

Looking to the above possibilities and the XRD results obtained for $In_{0.2}Sb_{1.8}Te_3$ it is quite clear that In substitutes Sb or Te.

The decrease in the band gap of $In_{0.2}Sb_{1.8}Te_3$ can be explained on the basis of the assumption that the effect is associated with the substitution of Sb in Sb_2Te_3 by In forming uncharged In_{Sb}^{x} defect as explained by Horak et al[10] but with a simultaneous replacement of Te^2 by Sb forming stable InSb-Sb_2Te_3 solid solution wherein the displaced atom of Te^2 is soluble. This phenomenon can schematically be represented as below:

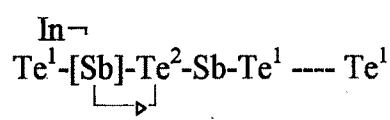

Since the band gap of InSb is 0.16 eV[30], the band gap of its solid solution with Sb_2Te_3 as per the simple model of substitution is expected to have the band gap intermediate to the values for two stable binary compounds, i.e., InSb and Sb_2Te_3. Hence the reduced band gap result of $In_{0.2}Sb_{1.8}Te_3$ is explained not on the basis of solid solution of In_2Te_3-Sb_2Te_3 but on the basis of formation of continuous InSb-Sb_2Te_3 solid solutions. This result is supported by the XRD reports wherein no In or InSb peaks are identified which could indicate that Sb is substituted by In in Sb_2Te_3 system.

Since the band gaps of $Bi_xSb_{2-x}Te_3$ (x = 0, 0.2, 0.5, 1) and $In_{0.2}Sb_{1.8}Te_3$ obtained in the present study are in the range of 0.2eV – 0.3 eV as also reported by different authors[12,13,31] for Sb_2Te_3 system, it seems reasonably certain that the band structure involved is the same for these compounds. Mooser and Pearson[32] have discussed empirical correlations between E_g and several parameters, such as lattice constant and heat of formation, for several compound-semiconductor series. Through alloying and pressure studies of this series of rhombohedral compounds and their alloys, it should be possible to correlate the effects of change in bond length, change in bond angle and relative electronegativity of different atoms with the change in E_g for a particular band structure. However, sufficient information regarding these aspects is not available as yet to establish correlations which would identify significant variables affecting E_g in alloys of these substances.

CONCLUSION

1) The band gap of $Bi_xSb_{2-x}Te_3$ (x = 0, 0.2, 0.5, 1) and $In_{0.2}Sb_{1.8}Te_3$ are all direct and no indirect transitions are observable.
2) The band gap of $Bi_xSb_{2-x}Te_3$ (x = 0, 0.2, 0.5, 1) has been observed to decrease with x varying from 0 to 1. The result is in fair agreement with the simple model of substitutional solid solution where we observe the band gap lying between the the values of E_g of the pure binary crystals i.e. Sb_2Te_3 and Bi_2Te_3.
3) The reduction in band gap of In incorporated Sb_2Te_3 is attributed to the effect caused by the substitution of Sb by In and of Te by Sb which in turn must have resulted in the formation of InSb – Sb_2Te_3 alloy.

REFERENCE

[1] Braunstein, R., Moore, A. R. and Herman, F. (1958) Phys. Rev. 109, 695.

[2] Larach, S., Shrader, R. E. and Stocker, C. F. (1957) Phys. Rev. 108, 587.

[3] Harman, T. C., Kleiner, W. H., Strauss, A. J., Wright, G. B., Mavroides, J. G., Honig, J. M. and Dickey, D. H. (1964) Solid State Commun. 2, 305.

[4] Jeon, H. W., Ha, H. P., Hyun, D. B. and Shim, J. D. (1991) J. Phys. Chem. Solids 52,579.

[5] Rosi, F. D., Hockings E. F. and Lindenblad, N. E. (1961) RCA Rev. 22, 82.

[6] Testardi, L. R., Bierly, Jr. J. N. and Donahoe, F. J. (1962) J. Phys. Chem. Solids 23, 1209.

[7] Champness, C. H. Chiang, P. T. and Parekh, P. (1965) Can. J. Phys. 43, 653.

[8] Rosenberg, A. J. and Strauss, A. J. (1961) J. Phys. Chem. Solids 19, 105.

[9] Horak, J., Lostak, P. and L. Benes (1984) Phil. Mag. B 50, 665.

[10] Horak, J., Stary, Z., Lostak, P. and Pancir, J. (1988) J. Phys. Chem. Solids, 49, 191.

[11] Jaschke, R. (1964) Ann. Physik, 15, 1, 106.

[12] Black, J., Conwell, E., Seigle, L. and Spencer, C. W. (1957) J. Phys. Chem. Solids 2, 240.

[13] Sehr, R. and Testardi, L. R. (1962) J. Phys. Chem. Solids 23, 1219.

[14] Poretskaya, L. V., Abrikosov, N. Kh. And Glazov, V. M. (1963) Zh. Neorg. Khim. 8, 1196.

[15] Rosi, F. D., Abeles, B. and Jengen, R. V. (1959) J. Phys. Chem. Solids 10, 191.

[16] Testardi, L. R. and Wiese, J. R. (1961) Trans. Met. Soc. AIME 221, 647.

[17] Airapetiants, S. V. and Efimova, B. A. (1958) Zhur. Tekh. Fiz. 28, 1768.

[18] Smith, M. J., Knight, R. J. and Spencer, C. W. (1962) J. Appl. Phys. 33, 2186.

[19] Kohler, H. and Freudenberger, A. (1977) Phys. Stat. Sol. (b) 84, 195.

[20] Stolzer, M., Stordeur, M., Sobotta, H. and Riede, V. (1986) Phys. Stat. Sol. (b) 138, 259.

[21] Kroutil, J., Navratil, J. and Lostak, P. (1992) Phys. Stat. Sol. (a) 131, K73.

[22] Lostak, P., Novotny, R., Kroutil, J. and Stary, Z. (1987) Phys. Stat. Sol (a) 104, 841.

[23] The Michelson Series FT-IR Spectrometer, Users Guide, Version 1.51, September 1993. BOMEM, Canada.

[24] Mott, N. F. and Jones, H. (1936) " Theory of the Properties of Metals and Alloys," Oxford Univ. Press, London and New York, 116.

[25] Chalmers, R. G. (1950) Nature 165, 239.

[26] Biondi, M. A. (1956) Phys. Rev. 102, 964.

[27] Stordeur, M., Langhammer, H. T., Sobotta, H. and Riede, V. (1981) Phys. Stat. Sol. (b) 104, 513.

[28] Li. C. Y., Ruoff, A. L. and Spencer, C. W. (1961) J. Appl. Phys. 32, 1733.

[29] Harbecke, G. and Lautz, G. (1958) Z. Naturf. 9a, 775.

[30] Sze, S. M. (1979) Physics of Semiconductor Devices, Wiley Eastern Ltd., New Delhi, 20.

[31] Horak J., Tichy L., Vasko A. and Frumar M. (1972) Phys. Stat. Sol. (a) 14, 289.

[32] Mooser, E. and Pearson W. B. (1960) Progress in Semiconductors, Heywood and Company, London, 5, 103.